

Electronic Supporting Information
Compositional Engineered Cd-Mo-Se Alloyed QDs toward
Photocatalytic H₂O₂ Production and Cr (VI) Reduction with Detailed
Mechanism and Influencing Parameters

Jyotirmayee Sahu, Sriram Mansingh, Bhagyashree Priyadarshini Mishra, Deeptimayee Prusty, and
Kulamani Parida*

Centre for Nanoscience and Nanotechnology, Siksha 'O' Anusnadhan (Deemed to be
University), Bhubaneswar-751030, Odisha (India)

*Corresponding author

E-mail: paridakulamani@yahoo.com &

kulamaniparida@soa.ac.in

Characterization:

Physical characterizations:

To investigate the crystallographic structure and phase purity of the synthesized sample X-ray diffraction (XRD) pattern was collected on a Rigaku Miniflex Ultima IV with Cu K α radiation (power rating: 100mA, 40kV, and $\lambda=1.54\text{\AA}$). The morphological analysis of the as-synthesized photocatalysts was carried out by using HR-TEM 300 kV of model Tecnai G2, F30 for the HRTEM study. UV-Vis diffuse reflectance spectroscopy was obtained using a JASCO-V-750 UV-visible spectrophotometer. Photoluminescence (PL) spectroscopy was used to investigate the recombination rate and separation efficiency of quantum dots at ambient temperature using a JASCO FP-8300 spectrofluorometer with an excitation wavelength of 380 nm. The surface chemistry and elemental composition of the photocatalysts are examined by XPS using a Karto axis ultra-x-ray photoelectron spectrometer, which is equipped with a monochromatized X-ray source (Al K α). Photoelectrochemical measurements, using an IVIUMSTAT multichannel workstation were performed where a conventional three-electrode Pyrex cell with Pt and Ag/AgCl respectively as counter and reference electrodes. An electrophoretic deposition (EPD) method was employed to prepare a working electrode, in which photocatalysts were deposited on Fluorine doped tin oxide (FTO). Typically, in a beaker, 20 mg of photocatalyst with 20 mL of acetone and iodine were taken and then the solution was dispersed by sonication for 10 min. In the above well-dispersed solution two parallel FTOs (separated by 10-15 mm) were dipped, and under controlled potentiostatic condition, 60 V bias was subjected (5 min) to coat the FTO surface by the photocatalyst as a thin film in 1 cm² area. The photocatalyst was deposited on FTOs and kept in the oven for 6 h to remove impurities from the FTO surface. Linear sweep voltammetry (LSV) was executed at a scan rate of 25 mV/s applying a potential of 0 to -0.8 V. Electrochemical impedance spectroscopy was also performed at zero biased potential at frequencies 10⁻¹ to 10⁵ Hz. In dark conditions, the Mott-Schottky analysis was also carried out. All the above electrochemical analyses were carried out using 0.1 M Na₂SO₄ solution.

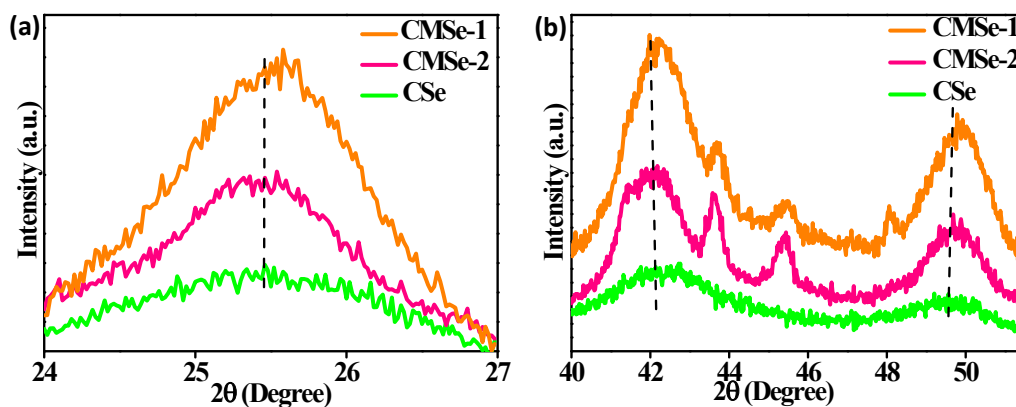


Figure S1. Enlarged view of XRD of CMSe-1 and CMSe-2 concerning binary CdSe QD to show shifting (a) at 25.5° and (b) at around 42 ° and 49°.

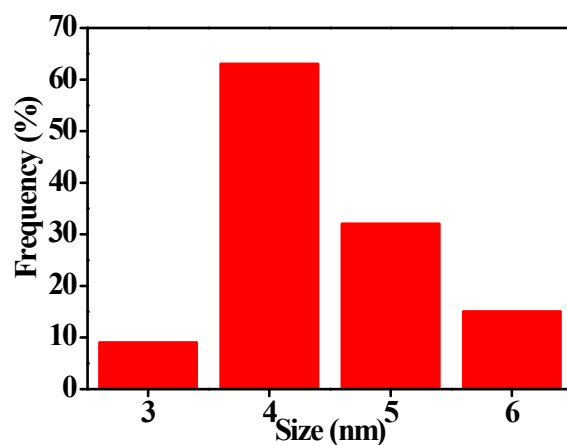


Figure S2. Particle size distribution of CMSe-1 QDs.

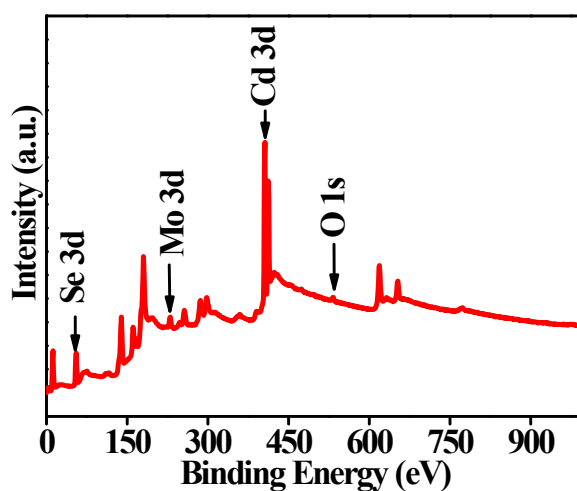


Figure S3. XPS survey of CMSe-1.

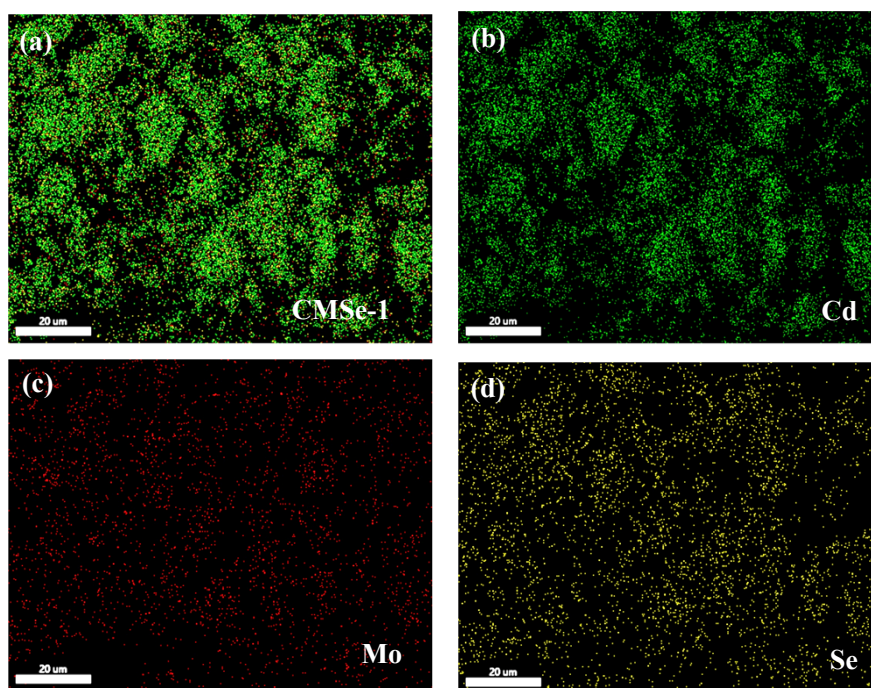


Figure S4. Elemental colour mapping image of (a) CMSe-1, (b) Cd, (c) Mo, and (d) Se elements.

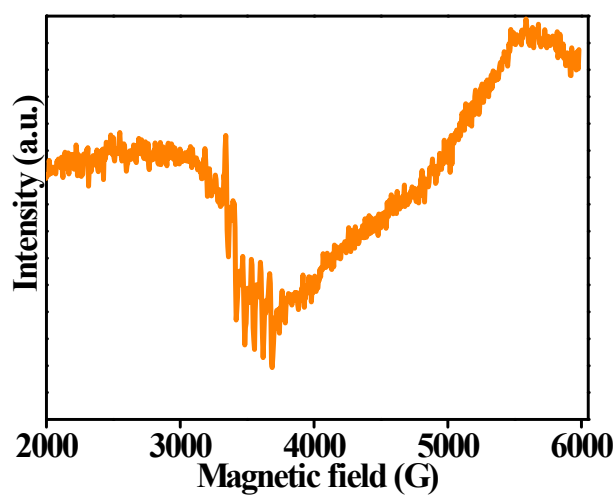


Figure S5. EPR spectra of CMSe-1

Table S1. Biexponential-Curve-Fitted TRPL parameters of CMSe-1 and CMSe-2 QD.

| Photocatalyst | α_1 | τ_1 (ns) | α_2 | τ_2 (ns) | τ_{avg} (ns) |
|---------------|------------|---------------|------------|---------------|--------------------------|
| CMSe-1 | -205.6427 | 1 | 230.8681 | 1.1 | 1.53 |
| CMSe-2 | -81.4482 | 1 | 91.8009 | 1.1 | 1.51 |

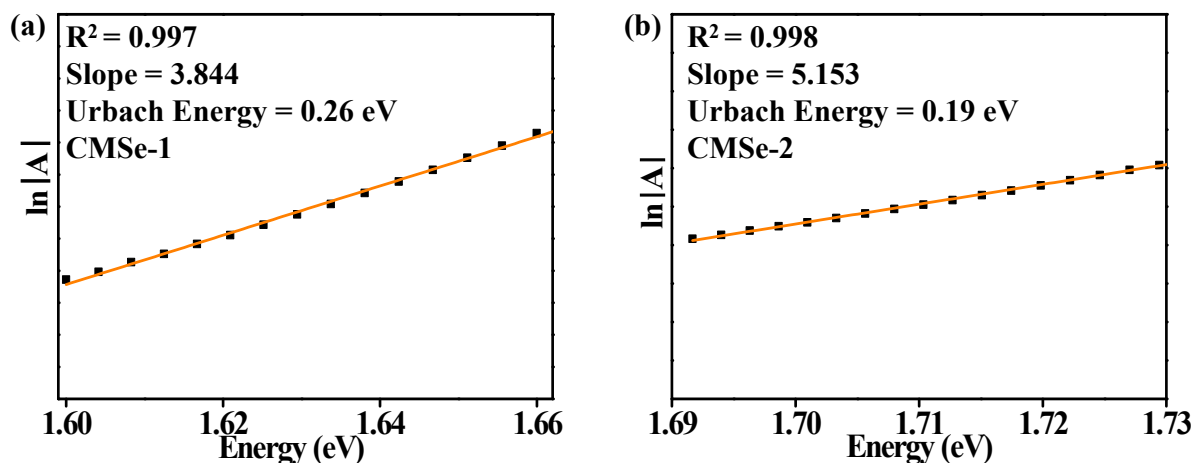


Figure S6. Urbach energy of (a) CMSe-1, and (b) CMSe-2 QD.

Calculation of solar to chemical conversion efficiency (SCC %)

SCC % of CMSe-1 QDs towards H_2O_2 production under 250 W Hg-lamp can be calculated by following the equation below:

$$SCC = \frac{\Delta G^\circ \text{ for } H_2O_2 \text{ Production} \times H_2O_2 \text{ produced (mol)}}{\text{Input energy (W)} \times \text{reaction time (sec)}} \times 100 \quad S1$$

Furthermore, ΔG° for H_2O_2 evolution is 117 kJ.mol^{-1} . The irradiance of 250 W Hg-lamp is 1.33 W.cm^{-2} and 127.2 cm^2 irradiated area. In a 1 h of reaction time, the amount of H_2O_2 produced is $28.06 \text{ }\mu\text{mol}$.

$$\begin{aligned} \text{Input energy (W)} &= \text{irradiance (Wcm}^{-2}) \times \text{irradiated area (cm}^2) \\ &= 1.33 \times 127.2 \\ &= 169.14 \end{aligned}$$

According to equation (1), the SCC efficiency is determined to be 0.27%.

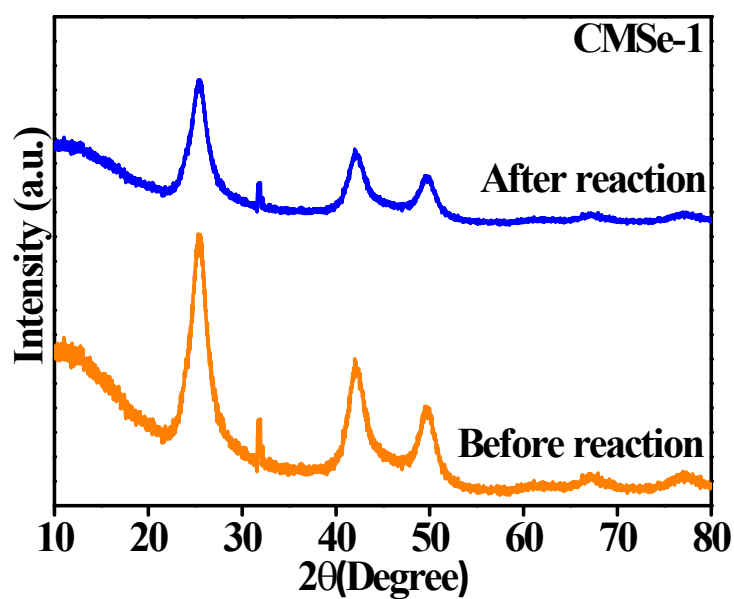


Figure S7. Powder XRD of CMSe-1 after performing photocatalytic activity.

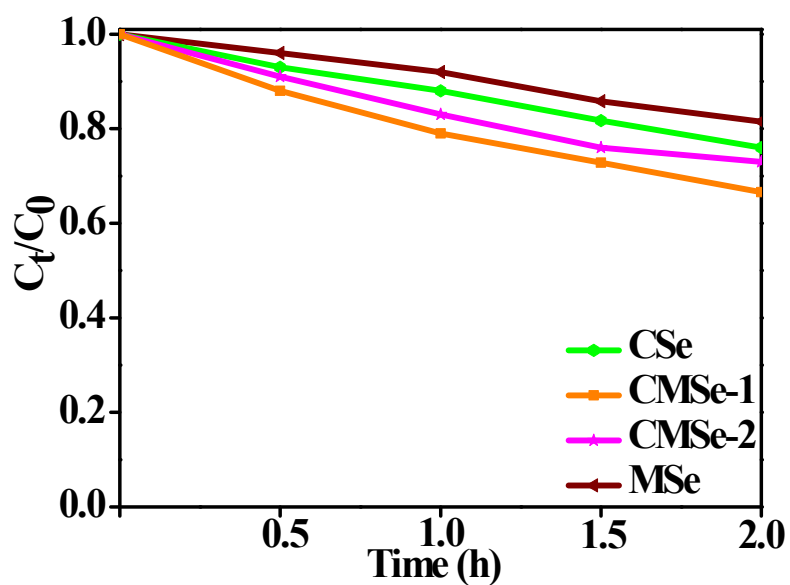


Figure S8. Photocatalytic decomposition of H_2O_2 by CMSe-1, CMSe-2, CSe, and MSe under visible light irradiation.

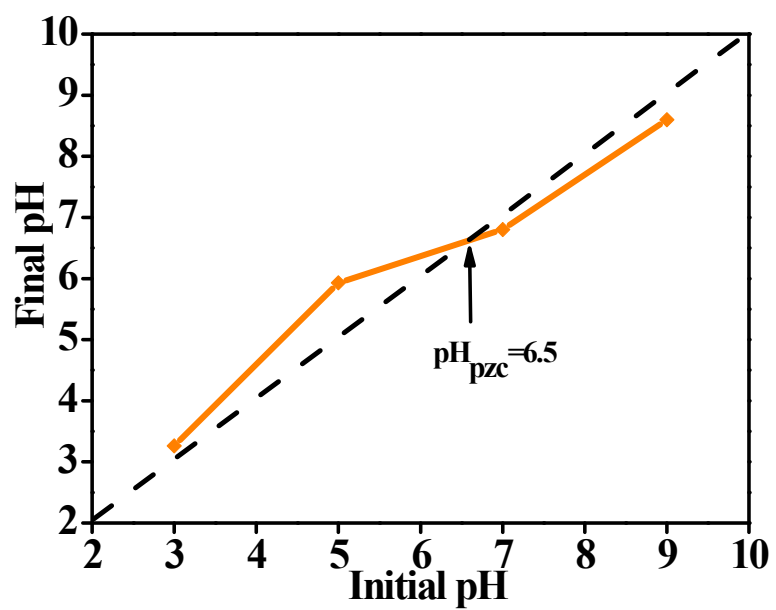


Figure S9. The pH_{pzc} value of CMSe-1 QD.

Figure S10. NBT test for detection of superoxide radicals of CMSe-1 and CMSe-2 QDs.

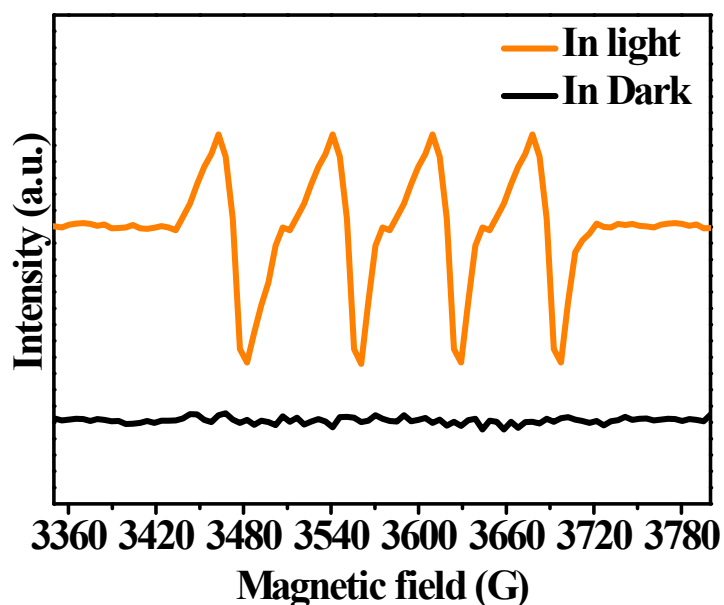


Figure S11. DMPO-ESR spin trapping spectra of CMSe-1 for detection of superoxide radical ($\cdot\text{O}_2^-$)

Table S2. Comparison Study on H_2O_2 Production and Cr (VI) Reduction over other photocatalysts.

| Photocatalyst | Rate Of H_2O_2 production | Efficiency of Cr (VI) reduction | Ref. |
|--|--|---------------------------------|-----------|
| $\text{CdSe}_{550}/5\text{CdS}/2\text{ZnS}$ QD | 126 mmolL^{-1} in 2 hours | - | 1 |
| CdSe QD/KPN-HCP | $900 \text{ } \mu\text{mol g}^{-1}$ in 1hour | - | 2 |
| CdSe/Se/BiOBr | $4180 \text{ } \mu\text{mol L}^{-1}$ in 4h | - | 3 |
| $\text{CdS}/\text{Ti}_3\text{C}_2\text{T}_x$ | $401 \text{ } \mu\text{mol L}^{-1}$ within 1 h | | 4 |
| $\text{ZnS}/\text{ZnSe}/\text{MoSe}_2$ | - | 96 % for 1.5 h | 5 |
| $\text{MoS}_2\text{-PVP}$ | - | 99.5 % for 3 h | 6 |
| CQD/ MoSe_2 | - | 99% for 3 h | 7 |
| $\text{CdS}/\text{Bi}_2\text{MoO}_6$ | - | 97% for 1 h | 8 |
| CMSe-1 | $1403.5 \text{ } \mu\text{molg}^{-1}\text{h}^{-1}$ | 93.6% in 2 hours | This work |

References:

1. W. Ji, Z. Xu, S. Zhang, Y. Li, Z. Bao, Z. Zhao, L. Xie, X. Zhong, Z. Wei and J. Wang, , *Catal. Sci. Technol.*, 2022, **12**, 2865-2871.
2. J. Xu, Q. Ji, Y. Wang, C. Wang and L. Wang, *Chem. Eng. J.*, 2021, **426**, 130808.
3. C. Du, S. Nie, C. Zhang, T. Wang, S. Wang, J. Zhang, C. Yu, Z. Lu, S. Dong, J. Feng and H. Liu, *J. Colloid Interface Sci.*, 2022, **606**,1715-1728.

4. Z. Yang and J. Wang, *ACS Appl. Nano Mater.*, 2022, **6**, 558-572.
5. L. Qiu, Y. Wang, X. Zhang, F. Tian, C. Zhu, J. Sheng, W. Yang and Y. Yu, *ACS Appl. Nano Mater.*, 2022, **6**, 523-532.
6. Y. Zhang, H. Li, X. Zhang, H. Zhang, W. Zhang, H. Huang, H. Ou and Y. Zhang, *J. Colloid Interface Sci.*, 2023, **630**, 742-753.
7. Z. Ren, X. Liu, H. Chu, H. Yu, Y. Xu, W. Zheng, W. Lei, P. Chen, J. Li and C. Li, *J. Colloid Interface Sci.*, 2017, **488**, 190-195.
8. D. Kandi, S. Martha, A. Thirumurugan and K. M. Parida, *ACS Omega*, 2017, **2**, 9040-9056.